**Journal of Korean Powder Metallurgy Institute**
Vol. 8, No. 3, 2001

# Multifunctionality in Ceramic/Metal Nanocomposites

**Tohru Sekino, Hiroki Kondo and Koichi Niihara**
*The Institute of Scientific and Industrial Research, Osaka University, Osaka 567-0047, Japan*
(Received August 30, 2001)

**Abstract** Several fabrication processes, corresponding nanostructural features and multifunctionality as well has been investigated for oxide ceramic based nanocomposites with metal nanodispersion (i.e., ceramic/metal nanocomposites). Transition metal (Ni, Co, etc) dispersed alumina and zirconia based nanocomposites have been synthesized by reducing and hot-press sintering of ceramic and metal oxide mixtures prepared by several method. Improved fracture strength (1.1 and 1.9 GPa for $Al_2O_3$/Ni and $ZrO_2$/Ni nanocomposites, respectively) of these composites have been achieved according to their nanostructures. In addition, ferromagnetic characteristic has been kept. The variation of magnetization with an applied stress has found to be more sensitive as smaller as the magnetic metal dispersion is. This result thus suggests the possibility of fracture and/or stress sensing of the composites by simple magnetic measurement.

**Keywords :** Ceramic/metal nanocomposites, Mechanical properties, Ferromagnetic, Stress sensing, Multifunctionality

## 1. Introduction

Nanostructured material such as nanocomposite and nanophase materials is one of the promising materials to overcome several engineering, environmental and/or economical problems. In the case of ceramic-based nanocomposites, excellent enhancement of mechanical properties have bee achieved by dispersing nanometer-sized second phase dispersion into several ceramic matrices such as $Al_2O_3$, MgO, $Si_3N_4$ and so on.[1] For instance short-crack toughening was found to be dominant in the $Al_2O_3$/SiC nanocomposites,[2] and such nanodispersion contributed on the inhibition of grain boundary sliding at elevated temperature, resulted in the improvement high-temperature strength and creep resistance.[3] In addition, new functions like superplasticity[4,5] and/or machinability[6,7] with excellent mechanical properties has also been verified due to their unique nanostructures. These results imply us that multi-functionalization can be achieved by the nanostructure control of ceramics.

Based on this materials design concept we have focused on the development of nanosized metal dispersed ceramic composites (i.e., ceramic/metal nanocomposites) in alumina/tungsten,[8-10] alumina/nickel,[11] alumina/molybdenum,[12] zirconia/molybdenum[13] and alumina/copper[14,15] systems and so on. For the ceramic /metal nanocomposites, addition of new functions such as magnetic and/or electric characteristics and resultant multi-functionalization would be expected due to the functionality of dispersed nano-sized metal. To achieve such a multifunctionality in nanocomposites, development and optimization of materials processing for suitable nanostructures as well as understanding of the roles of nanostructure on properties will be required. Reduction and subsequent hot-press sintering method[8-11] was used to prepare in-situ metal dispersed ceramic materials, where corresponding oxides were mixed with ceramic powders.

In this paper, several fabrication processes, corresponding nanostructural features and multifunctionality will be introduced for the alumina and zirconia based nanocomposites with magnetic metal (Ni and Co) nanodispersion.

## 2. Experimental Procedure

High-purity cobalt nitrate ($Co(NO_3)_2 \cdot 4H_2O$) or nickel nitrate ($Ni(NO_3)_2 \cdot 6H_2O$) was selected as a source of metal dispersion. Weighted nitrate (0 to 20 vol% metal in final composites) was dissolved in alcohol, and $\alpha$-$Al_2O_3$ powder (0.2 μm) or 3 mol% $Y_2O_3$ stabilized $ZrO_2$ powder (3Y-TZP, 150 nm) was mixed by ball milling. Dried mixtures were calcined in

air to obtain ceramic/metal-oxide mixtures such as $Al_2O_3$/NiO. The composite systems investigated in this study are thus $Al_2O_3$/Ni, $Al_2O_3$/Co and t-$ZrO_2$/Ni (Y-TZP/Ni). The obtained mixtures were reduced by $H_2$ gas from 700 to 900°C, then hot-press sintering was successively accomplished at 1400°C to 1600°C for 1 h in Ar atmosphere under an applied pressure of 30 MPa.[10,11]

Crystalline phase of the obtained specimens was characterized by the XRD with CuKα radiation. Transmission electron microscopy (TEM) was used to observe powder morphology and microstructure of the prepared material. The fracture toughness was estimated by the indentation fracture (IF) method, and partly by the indentation strength in bending (ISB) technique. The fracture strength measurement was carried out by 3-point bending test with 30 mm span. The magnetization of the composite was estimated by the vibrating sample magnetometer (VSM) with an applied magnetic field up to ±9 kÖe at room temperature. Variation of magnetization with an applied uniaxial stress was measured at room temperature.

## 3. Results and Discussion

### 3.1. Powder morphologies

Morphology and crystalline phase of the powder mixtures have varied depending on the heat treatment. Fig. 1 shows the variation of powder morphology during powder processing for $Al_2O_3$/Ni nanocomposites, where nickel nitrate was used. TEM investigation revealed that the nitrate, which was coated on the $Al_2O_3$ primary particles as a shapeless matter after drying of the mixtures (Fig. 1a), was changed to be spherical nanoparticles of approximately 20 to 40 nm precipitating around $Al_2O_3$ particles after calcining in air (Fig. 1b). The nickel oxide maintained the size and structure even after the hydrogen treatment at 700°C as is seen in Fig. 1(c). Similar feature was also confirmed for $Al_2O_3$/Co system. Complete reduction of $Co_3O_4$ and NiO to corresponding metals was also confirmed by the XRD analysis. In the case of $ZrO_2$/Ni system, however, agglomeration of produced nano-sized NiO was found in the calcined powders. This difference is probably due to the different characteristics of powder surface between $Al_2O_3$ and $ZrO_2$ and/or the different affinity to NiO.

On the contrary to the ceramic/oxide mixtures obtained by using nitrate, the average particle size of oxide was in submicron range, around 100 to 300 μm, in the ball-milled ceramic/oxide powders. It is thus considered that chemical preparation process provides more suitable powder mixtures for the ceramic/metal nanocomposites.

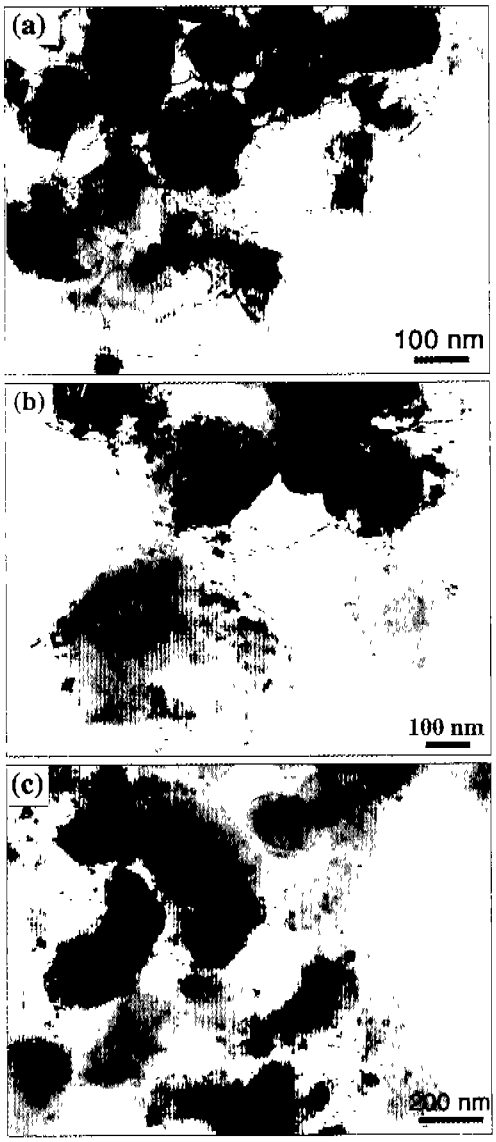


**Fig. 1. Variation of powder morphology during processing for $Al_2O_3$/Ni nanocomposites. (a) dried $Al_2O_3$/$Ni(NO_3)_2$ $6H_2O$ mixture, (b) calcined powder (nano-sized NiO formed on the alumina particles), and (c) reduced powder (nano-sized Ni particles existed with maintaining their size).**

### 3.2. Microstructure and interface characteristics

Prepared $Al_2O_3$/NiO, $Al_2O_3$/$Co_3O_4$ and $ZrO_2$/NiO

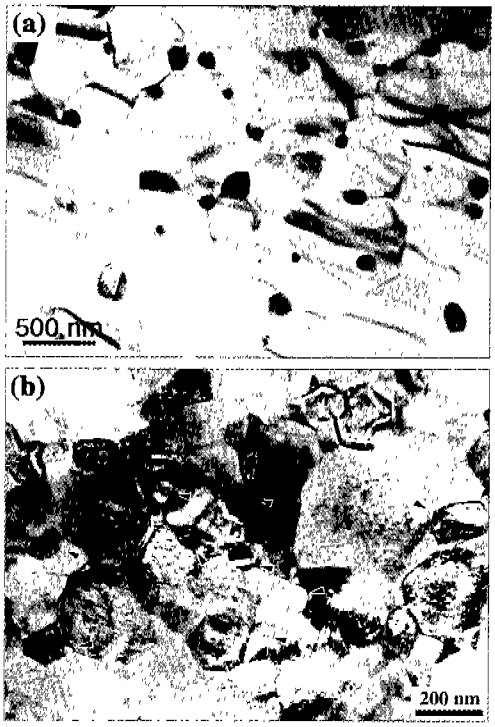


**Fig. 2. TEM micrographs of $Al_2O_3$/5 vol% Ni nanocomposite (a) and Y-TZP/5 vol% Ni nanocomposite (b) prepared by using nickel nitrate as a source material of metal dispersion.**

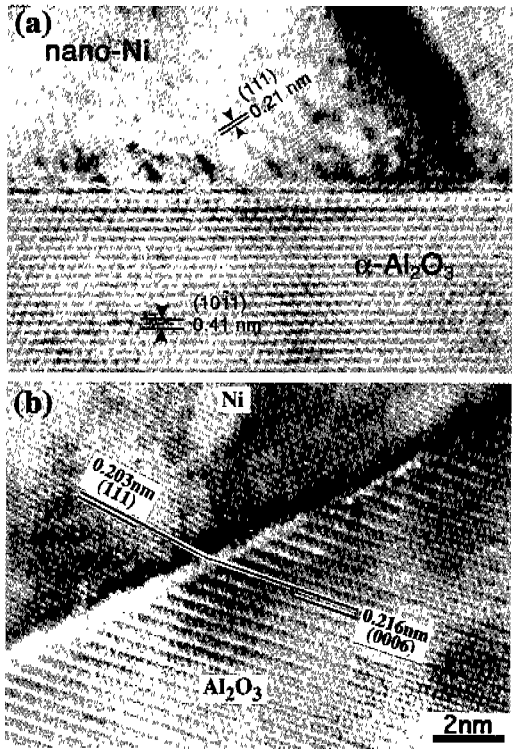


**Fig. 3. Interface between nano-sized Ni and $Al_2O_3$ grain observed in the specimen from nitrate (a) and between micron-sized Ni and $Al_2O_3$ (b) found in $Al_2O_3$/Ni sintered using commercial NiO.**

mixtures were then reduced by $H_2$ gas at less than 900°C, and successively hot-press sintered at 1400 to 1500°C for 1 h in Ar atmosphere with an applied pressure of 30 MPa. After sintering, the specimens were composed of only α-$Al_2O_3$ and Ni or Co, and tetragonal $ZrO_2$ and Ni for each system. Neither residual transition metal oxide nor reaction phase was observed. Theoretical densities of over 98% were observed for all of the specimens.

TEM investigation revealed that nano-sized Ni particles around 100 nm or less were found to dispersed at the grain boundary and/or triple-point junctions in alumina and zirconia matrices, showing intergranular-type of nanostructure (see Fig. 2). This is different from the alumina/tungsten nanocomposites prepared by the reduction and sintering technique.[10] By comparing the size of dispersed Ni in $Al_2O_3$ between the samples prepared by using NiO and nickel nitrate, finer dispersion was obtained for the latter specimens (nitrate used), which well agreed with the powder morphology before sintering as mentioned above.

When metal was dispersed into alumina, the particles tended to grow during sintering with increasing its volume fraction, especially for $Al_2O_3$/Co system. In the case of Y-TZP/Ni system, matrix grain size of zirconia was also fine in sub-micron range, typically 300 nm as is shown in Fig. 2(b).

Heterogeneous interface between oxide matrix and metal dispersion is considered to have important role. Fig. 3(a) represents high-resolutional image between Ni nanodispersion and $Al_2O_3$ grain. No intermediate phase was found but facet plane was observed, which was based on the low Miller index plane of corundum structure such as (1011). It is thus considered that formation of coherent and straight hetero-interface, which was governed by the formation of Wulff structure of $Al_2O_3$, and resultant relaxation of lattice and thermal expansion mismatches might stabilize the nanostructure in the present composite system. On the other hand, disturbed interface was seen between alumina and large Ni particle located at the grain

**Table 1. Fracture strength and toughness for ceramic/metal composites prepared by using metal oxide and nitrate as raw materials.**

| System | Source of metal dispersoid | Metal content (vol%) | Fracture toughness (MPa-$m^{0.5}$) | Fracture strength (MPa) |
|---|---|---|---|---|
| $Al_2O_3$ | - | 0 | 3.22 ± 0.38 | 702 ± 53 |
| $Al_2O_3$/Ni | NiO | 5 | 3.52 ± 0.10 | 980 ± 6 |
| | NiO | 20 | 4.50 ± 0.10 | 714 ± 35 |
| $Al_2O_3$/Ni | $Ni(NO_3)_2$ | 5 | 3.50 ± 0.10 | 1090 ± 53 |
| | $Ni(NO_3)_2$ | 20 | 4.01 ± 0.18 | 710 ± 25 |
| $Al_2O_3$/Co | $Co(NO_3)_2$ | 5 | 3.98 ± 0.24 | 955 ± 135 |
| | $Co(NO_3)_2$ | 20 | 5.23 ± 0.10 | 441 ± 24 |
| t-$ZrO_2$ | - | 0 | 5.41 ± 0.05 | 900 ± 75 |
| t- $ZrO_2$/Ni | NiO | 1 | 5.64 ± 0.11 | 1866 ± 10 |
| | NiO | 2 | 5.75 ± 0.08 | 1879 ± 56 |
| | NiO | 5 | 5.72 ± 0.05 | 1516 ± 121 |
| t- $ZrO_2$/Ni | $Ni(NO_3)_2$ | 5 | 5.69 ± 0.13 | 1092 ± 34 |
| | $Ni(NO_3)_2$ | 10 | 5.21 ± 0.01 | 1238 ± 120 |
| | $Ni(NO_3)_2$ | 20 | 4.92 ± 0.29 | 1585 ± 95 |

boundary (Fig. 3b), which seemed to be weaker interface. The ceramic-metal interfaces for the $Al_2O_3$/Co and Y-TZP/Ni systems were also clean without any reaction phase.

### 3.3. Mechanical properties

Mechanical properties for the ceramic/metal nanocomposites obtained in this investigation are summarized in Table 1. For all the composites, fracture strength was dominantly enhanced when small amount of metal dispersion, typically 5 vol% or less. Especially near 1.9 GPa of strength was achieved when very small amount of Ni (1 or 2 vol%) was incorporated into Y-TZP. Finer dispersion of Ni metal (i.e. metal dispersion from nitrate) into $Al_2O_3$ showed higher strength due to the refinement of the microstructure which strongly affected on the size of fracture origin.

Relationship between $Al_2O_3$ matrix grain size and strength for $Al_2O_3$/Ni and Co nanocomposites revealed that the nanocomposite showed higher strength than that of monolithic $Al_2O_3$ when the matrix size was in the same range (see Fig. 4). This result clearly suggests that another strengthening mechanism might exist in these composites.

By considering the difference of thermal expansion coefficient (TEC) between alumina ($8.3\times10^{-6}K^{-1}$) and metals (Ni; $13.3\times10^{-6}K^{-1}$, Co; $14.0\times10^{-6}K^{-1}$), tangential compressive force may be generated around metal dispersion by the mismatch. The fact that most metal particles located at the grain boundary thus

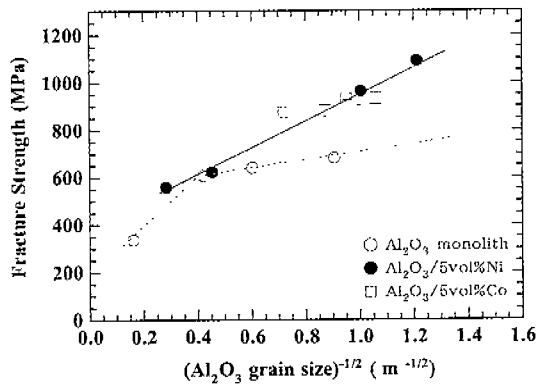


**Fig. 4. Relationship between average grain size of $Al_2O_3$ matrix and fracture strength for monolithic $Al_2O_3$, $Al_2O_3$/5 vol% Ni and $Al_2O_3$/5 vol% Ni nanocomposites sintered at the different temperature.**

implies that this force might strengthen the $Al_2O_3$-$Al_2O_3$ interface as is shown in Fig. 5, which also seems to contribute to the enhancement of the strength.

In the case of Y-TZP/Ni nanocomposites, however, the specimens prepared by using NiO indicated higher strength than that of nitrate used. The TEC of stabilized zirconia ($10\times10^{-6}K^{-1}$) is near to that of metal so that the residual stress may be minor contribution. The strengthening behavior is not clarified well yet but it seems to correlate with the small difference of the specimens density between them, the latter composite (nitrate used) was slightly lower relative density than

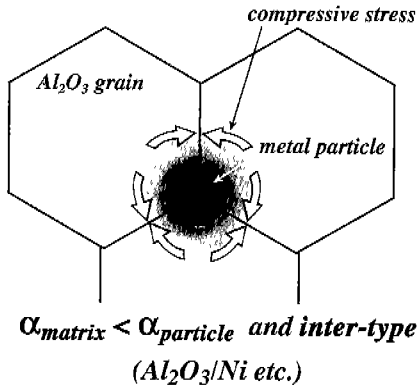


**Fig. 5. Schematic drawing for strengthening of grain boundary by thermal expansion mismatch between metal dispersoid and matrix.**

that of the former specimen.

On the contrary to the strength, the fracture toughness enhancement was not so much dominant. The most effective toughening mechanism in ceramic-metal composite is plastic deformation of metal phase, which can often be seen in cermet materials. In the present composites the size and fraction of metal phase are small so that the plasticity of metal phase is considered to be minor role on the toughening.

### 3.4. Magnetic properties providing multifunctionality

Prepared samples showed ferromagnetic behavior due to their magnetic metal dispersion. The magnetic coercive force, *Hc*, of Co and Ni dispersed in ceramic matrices is summarized in Table 2. *Hc* for the present nanocomposites is approximately one to two orders of magnitude larger than those of the corresponding pure metal. The increased coercive force of the present composites might be mainly attributed to the decreased particle size of isolated magnetic dispersions.

**Table 2. Magnetic properties for ceramic/metal nanocomposites.**

| Specimens | Coercive Force (Öe) | Particle size of metal (nm) |
|---|---|---|
| Co metal* | 10 | *annealed bulk* |
| $Al_2O_3$/5 vol%Co | 133 | < 550 |
| Ni metal* | 0.7 ~ 1 | *annealed bulk* |
| $Al_2O_3$/Ni | 51 | 98 |
| t-$ZrO_2$/5 vol%Ni | 138 | < 100 |

*reference data

*Hc* of magnetic particle is well known as a sensitive property to the particle size,[16] and also known to increase with decreasing of particle size due to the formation of magnetic single domain structure. By solving the minimum energy condition of total energy of magnetic material, critical particle size ($R_C$) of magnetic single domain of Ni was calculated to be about 80 nm.[16]

In addition, it is easily expected that internal stress affects on the magnetic domain wall formation, i.e. on the surface energy of magnetic domain wall, because it changes the energy for the system. Simple calculation in which the internal stress of 100 MPa was taken into account for $R_C$ of Ni particle suggested that the $R_{C,\,stressed}$ was approximately 1.5 times larger (thus around 160 nm) than that of isolated particle. In the present $Al_2O_3$/Ni and Y-TZP/Ni nanocomposites, the average size of Ni rigidly embedded within ceramic matrix is around 100 nm. This fact suggests that many particles are in the state of magnetic single domain which contributes on increasing of the coercive force of the nanocomposites.

Another important feature for these materials is the magnetization response to an applied stress. Magnetic material has anti-magnetostriction effect in which magnetization is changed to minimize total energy of magnetic matter when magnetic material is deformed (i.e. stress is applied). Fig. 6 represents the relationship between magnetization and an applied stress for Y-TZP/Ni composites, where Ni particle size is finer in Y-TZP/5 vol% Ni than in 20 vol% Ni specimen. As is seen clearly from the figure, the variation of magnetization with an applied stress is more sensitive as smaller as the magnetic metal dispersion is. Detailed

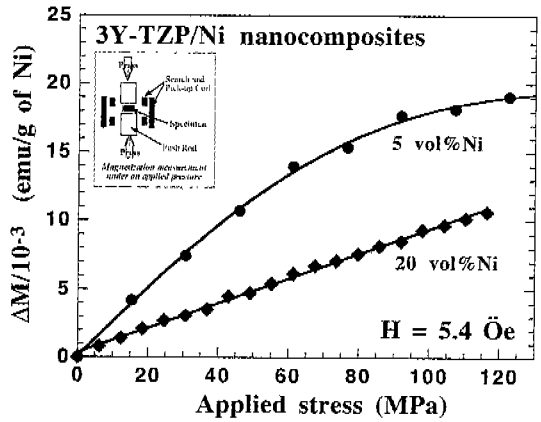


**Fig. 6. Relationship between magnetization change and an applied uniaxial stress of nickel in Y-TZP/Ni composites.**

mechanism of the enhanced response has not been clarified, however, it can be said that the nano-structuralization of magnetic metal within ceramic would make it possible to provide new function such as magnetic remote sensing capability[17] of nanocomposite material.

## 4. Conclusion

Nanometer-sized magnetic metal such as nickel and cobalt into oxide ceramics could be successively incorporated into alumina and tetragonal-zirconia ceramics by reduction and sintering of composite powders prepared by well-controlled processing. For $Al_2O_3$/Ni and Y-TZP/Ni nanocomposites, metal dispersion was kept to be less than 100 nm and located mainly at grain boundaries. Consequently, the enhancement of mechanical properties was achieved. Especially improved fracture strength of approximately 1.1 and 1.9 GPa for $Al_2O_3$/Ni and $ZrO_2$/Ni nanocomposites, respectively, was observed when metal fraction was small, less than 5 vol%.

In addition, ferromagnetic nature was also found to be compatible with the excellent mechanical properties. Magnetic coercive force was increased with decreasing of metal particle size due to the formation of magnetic single domain and the existence of internal stress. The variation of magnetization with an applied stress was more sensitive when the magnetic metal dispersion was finer, suggesting the possibility of fracture and/or stress sensing of the composites by simple magnetic measurement.

All these results imply that the nano-structuralization of ceramic and functional-metal would provide multifunctional composite materials with superior properties.

**Acknowledgements.** This work is partly supported by the Japan Society for the Promotion of Science (JSPS) Joint Research Projects under the Bilateral Programs between Japan and Korea. The authors acknowledge Professor Jai-Sung Lee of Hanyang University, Korea for the useful discussion.

## References

1. K. Niihara: J. Ceram. Soc. of Japan, **99** (1991) 974.
2. T. Ohji, Young-Keun Jeong, Yong-Ho Choa and K. Niihara: J. Am. Ceram. Soc., **81** (1998) 1453.
3. T. Ohji. T. Kusunose and K. Niihara: J. Am. Ceram. Soc., **81** (1998) 2713.
4. F. Wakai, Y. Kodama, S. Sakaguchi, N. Murayama, K. Izaki and K. Niihara: Nature, **344** (1990) 421.
5. Masashi Yoshimura, Tatsuki Ohji, Mutsuo Sando and Koichi Niihara: Mat. Res. Innov., **2** (1998) 83.
6. K. Suganuma, G. Sasaki, T. Fujita, M. Okumura and K. Niihara: J. Mater. Sci., **28** (1993) 1175.
7. T. Kusunose, Y. H. Choa, T. Sekino and K. Niihara: Key Eng. Mater., **161-163** (1999) 475.
8. T. Sekino and K. Niihara: Nanostr. Mater., **6** (1995) 663.
9. T. Sekino and K. Niihara: J. Mater. Sci., **32** (1997) 3943.
10. T. Sekino, J. -H. Yu, Y. -H. Choa, J. -S. Lee and K. Niihara: J. Ceram. Soc. Japan, **108** (2000) 541.
11. T. Sekino, T. Nakajima, S. Ueda and K. Niihara: J. Am. Ceram. Soc., **80** (1997) 1139.
12. M. Nawa, T. Sekino and K. Niihara: J. Mater. Sci., **29** (1994) 3185.
13. M. Nawa, K. Yamazaki, T. Sekino and K. Niihara: J. Mat. Sci., **31** (1996) 2849.
14. Sung-Tag Oh, T. Sekino and K. Niihara: Ceram. Eng. Sci. Proc., **18** (1997) 329.
15. Sung-Tag Oh, T. Sekino and K. Niihara: Nanostr. Mater., **10** (1998) 327.
16. A. Ye. Yermakov, O. A. Ivanov, Ya. S. Shur, R. M. Grechishkin and G. V. Ivanova: Phys. Met. and Metallogr., **33** (1972) 99.
17. M. Awano: Bull. Ceram. Soc. Jpn., (1997) 997.